

Tolerancing the alignment of large-core optical fibers, fiber bundles and light guides using a Fourier approach

TRAVIS W. SAWYER^{1,2,*}, RYAN PETERSBURG³, AND SARAH E. BOHNDIEK^{1,2}

¹Department of Physics, University of Cambridge, Cambridge, United Kingdom

²Cancer Research UK Cambridge Institute, University of Cambridge, Cambridge, United Kingdom

³Department of Physics, Yale University, New Haven, CT, 06511

*Corresponding author: ts661@cam.ac.uk

Compiled March 11, 2017

Optical fiber technology is found in a wide variety of applications to flexibly relay light between two points, enabling information transfer across long distances and allowing access to hard-to-reach areas. Large-core optical fibers and light guides find frequent use in illumination and spectroscopic applications; for example, endoscopy and high-resolution astronomical spectroscopy. Proper alignment is critical for maximizing throughput in optical fiber coupling systems, however, there currently are no formal approaches to tolerancing the alignment of a light guide coupling system. Here, we propose a Fourier Alignment Sensitivity (FAS) algorithm to determine the optimal tolerances on the alignment of a light guide by computing the alignment sensitivity. The algorithm shows excellent agreement with both simulated and experimentally measured values and improves on the computation time of equivalent ray tracing simulations by two orders of magnitude. We then apply FAS to tolerance and fabricate a coupling system, which is shown to meet specifications, thus validating FAS as a tolerancing technique. These results indicate that FAS is a flexible and rapid means to quantify the alignment sensitivity of a light guide, widely informing the design and tolerancing of coupling systems.

© 2017 Optical Society of America

OCIS codes: (060.2310) Fiber optics; (080.2208) Fabrication, tolerancing; (220.1140) Alignment

<http://dx.doi.org/10.1364/ao.XX.XXXXXX>

1. INTRODUCTION

Optical fibers are used in a wide range of modern technologies, including optical communications [1–3], astronomy [4–6], and biomedical optics [7–9] to flexibly transfer light between two points using total internal reflection (TIR). This technology proves to be an extremely useful tool for transferring information across long distances and accessing hard-to-reach areas, such as inside the human body. The simplest form of an optical fiber is a step-index fiber, which is composed of a plastic or glass core surrounded by a cladding material (Fig. 1a). If the index of refraction of the core medium is greater than the cladding, light propagation is supported for rays within the numerical aperture (NA) of the fiber [10]. In general, optical fibers can be classified as either single-mode or multi-mode. This distinction refers to the number of transverse modes that an optical fiber can support. A transverse mode is a spatial pattern of light, which arises during propagation due to the boundary condi-

tions imposed on the electromagnetic wave by the optical fiber (Fig. 1b) [11]. Multi-mode optical fibers can support multiple transverse modes, whereas a single-mode fiber can theoretically support a single mode only. The number of modes supported by a given fiber is dependent on operating wavelength, numerical aperture, and the core diameter [12].

As the core diameter of optical fibers is increased, the number of supported modes can increase drastically. Large-core optical fibers (LCOFs) and light guides are fibers with very large core diameters that can support hundreds if not thousands of modes. These fibers are often used for modal scrambling in astronomy [13], high-power laser transmission [14], and other applications. The term light guide can also refer to a fiber bundle, which are found frequently in illumination applications [15, 16] and endoscopy [17, 18]. Light pipes are similar devices, which also operate using the principle of TIR; however, in this case, the core element is on the scale of centimeters to meters. Air is typically used as a cladding medium for light pipes and the

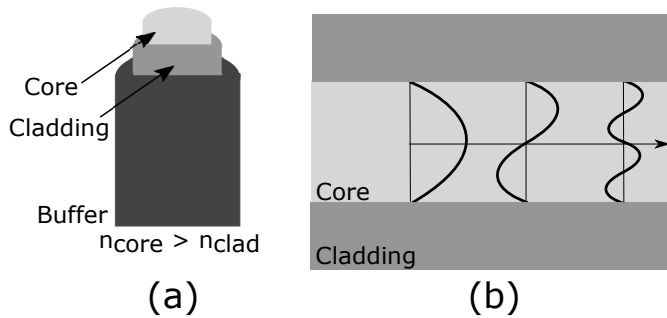


Fig. 1. Common architecture of a step-index optical fiber (a) and the presence of transverse modes (b), which arises in multimode fibers.

geometry can become highly freeform [19, 20]. These devices find widespread use in display technology and automotive lighting [21]. Where the behavior and properties of single-mode and multi-mode optical fibers can be described with mode calculation software [22], these computations become prohibitively expensive in the limit of many modes, as is the case with LCOF, fiber bundles, and light pipes. Different fields may use specialized terminology to differentiate between the various types of light transfer devices; for the remainder of this paper, the term light guide will be used to refer to any case where the optical fiber element possesses a sufficiently large diameter to produce enough modes to frustrate conventional optical fiber modal calculations.

For many light guiding applications, alignment is a critical aspect for achieving high throughput. This becomes particularly important when coupling to a focused light source; a minor misalignment may result in a high degree of loss as the focal point is translated off of the light guide and furthermore can influence the illumination distribution shape at the output. High throughput can influence exposure times, signal level, and overall image quality, making it an essential and important aspect of system performance. For single-mode and multi-mode fibers, mode coupling calculations can illustrate the performance for a given optical system; however, this approach is generally used to determine the modal power distribution and does not provide information about alignment sensitivity. Furthermore, mode coupling calculations do not scale well to light guide devices, where the number of modes is very large. Nevertheless, understanding alignment sensitivity is critical when designing coupling systems to determine the optimal tolerances for a given component to achieve the necessary throughput.

A potential solution to this challenge is to model the system of interest in an optical design and analysis software package and conduct ray tracing simulations to determine the sensitivity. For cases where the number of modes is very large, the light guide can effectively be modeled using geometrical optics, enabling the use of stochastic ray tracing methods implemented in many illumination software packages such as LightTools (Synopsis; Pasadena CA) and FRED (Photon Engineering; Tucson AZ). Such simulations are computationally expensive and interrogating alignment sensitivity requires a lengthy series of simulations to achieve the desired precision. Hence, an efficient, analytical approach could greatly inform the design of coupling systems. Recent advances in computer technology, particular in the scope of GPU computing, has the potential to dramatically increase raytracing speed [23, 24]. Even in this event, an analytical ap-

proach would provide a means to cross-check simulation results, a valuable and important practice in science and engineering.

Here we introduce a rapid analytical approach using Fourier theory to overcome this challenge. Previous work to analytically compute alignment sensitivity has been done for single-mode fibers; however, these approaches are limited by the use of traditional mode-coupling calculations and have not been extended to higher-moded devices [25, 26]. The Fourier Alignment Sensitivity (FAS) algorithm is a novel method to compute the alignment sensitivity for light guides, enabling the efficient determination of optimal tolerances for coupling mechanisms. We first present a mathematical description of the FAS algorithm, as well as the limitations and assumptions involved in its use. We then validate the algorithm by first comparing the results to ray tracing simulations and then by running laboratory tests of alignment sensitivity using light guides of varying sizes and shapes, including circular, rectangular and octagonal. Finally, the practical application of such a tool is demonstrated by designing an optical coupler using FAS to determine the optimal centration tolerances. We show that FAS is an accurate and rapid means to compute alignment sensitivity, which can be used to determine optimal tolerances. Furthermore, the results indicate that FAS is applicable to non-rotationally symmetric systems and is thereby highly robust and flexible. This implies that the proposed approach has potential to broadly inform optical system design and tolerancing.

2. THEORY

A. Fourier Alignment Sensitivity Algorithm

To understand the proposed analytical approach, consider first an irradiance distribution incident on a light guide (Fig. 2a). In the limit of geometrical optics, any light striking the core of the light guide, which is within the numerical aperture, will be propagated through the core due to TIR and transmitted through the device to the opposing face.

Misalignment of the light guide in a direction lateral to the optical axis will result in shifting the incident irradiance distribution relative to the core (Fig. 2b). As such, as the lateral misalignment is increased, the irradiance distribution will continue to shift off of the light guide core and less light will be transmitted until the distribution is fully vignetted by the light guide and no light enters the core. The relationship between the transferred power and lateral misalignment is defined here as the alignment sensitivity. Mathematically, determining the proportion of captured light corresponds to computing the overlap integral between the incident distribution and the input face of the light guide. While this shares similarities with a mode coupling calculation, in this case, the large number of modes are treated with geometrical optics as coalescing into the entrance aperture, represented by a top-hat function. To determine the alignment sensitivity, this calculation must be repeated for a range of lateral misalignments where, for each, the light guide is shifted laterally by some amount and the overlap between the incident irradiance distribution and the entrance aperture is computed. This process is described by the mathematical operation of cross-correlation. Thus, the captured power can be expressed as

$$P(x, y) = E(x, y) \star O(x, y), \quad (1)$$

where P is the transmitted power, x and y are the spatial coordinates corresponding to misalignment, $E(x, y)$ is the incident

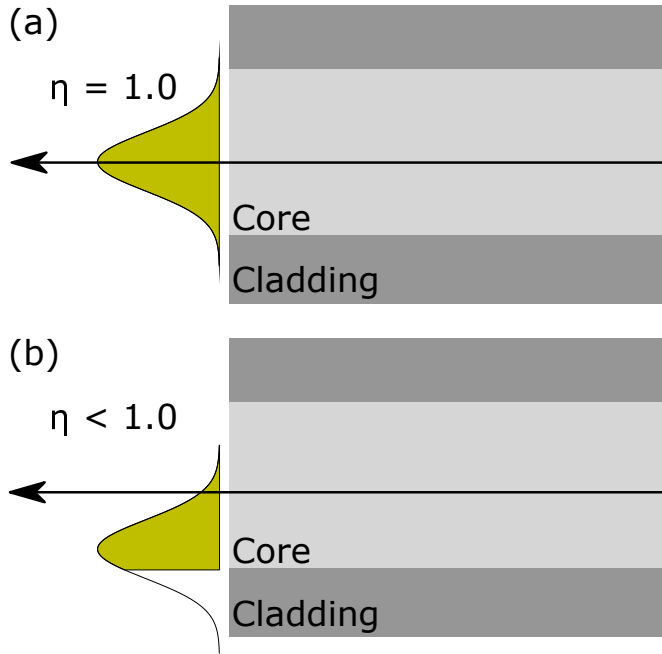


Fig. 2. An aligned light guide will capture the maximum power of a focused spot, integrating under the curve of the spot profile (a), which we define as an efficiency of one ($\eta=1$). A misaligned fiber (b) will lose energy, which does not enter the core.

irradiance distribution, $O(x, y)$ is the two-dimensional top-hat function representing the light guide input face, and \star denotes the cross-correlation operation. By normalizing E to integrate to one, Eq. (1) can be transformed to

$$\eta(x, y) = \hat{E}(x, y) \star O(x, y), \quad (2)$$

where $\eta(x, y)$ is the transfer efficiency as a function of lateral misalignment in x and y , which corresponds to the alignment sensitivity. Cross-correlation can be computationally expensive; by invoking the convolution theorem, Eq. (2) can be computed directly using the Fourier Transform as

$$\eta(x, y) = \mathcal{F}^{-1}\{\mathcal{F}[\hat{E}(x, y)][\mathcal{F}[O(x, y)]]\}. \quad (3)$$

By expressing the alignment sensitivity in terms of the Fourier Transform, the numerical computation can be done using the Fast Fourier Transform algorithm, which is markedly faster than cross-correlation and scales more tractably to larger datasets [27].

B. Limitations of Proposed Approach

We identify a number of limitations associated with the proposed algorithm. First is the assumption that the light guide supports a large number of transverse modes. The precise limit at which the algorithm is valid is not known and remains an objective of future research. To determine this, alignment sensitivity measurements would need to be made on light guides of increasing mode number and compared with the algorithm results in each case. This is beyond the scope of this paper and remains a long-term goal. A further approximation is that all energy entering the core is within the numerical aperture of the light guide and is supported for propagation. In practice, assuring that all light is within the numerical aperture of the system can be controlled by selecting appropriate optics, thus

validating this assumption; however, if this constraint is broken, the observed losses would increase. Another approach is to compute the overlap integral of the fiber numerical aperture with that of the beam. This would provide another efficiency term to scale Eq. (3) and could potentially extend the algorithm to investigate angular alignment sensitivity, which is an aim of ongoing work. Furthermore, some cladding transmission may occur, particularly for light guides of short lengths, which would increase the observed transmission. We demonstrate that we can account for such effects by altering the shape of the top-hat function to have multiple levels of transmission for the core and cladding.

In practice, each interface will also induce Fresnel reflections and the core material will possess some intrinsic absorption, leading to losses in the transmitted power. Considering this, the alignment sensitivity represents a relative quantity and does not include these additional losses without a further scaling of the result.

3. METHODS

A. Simulated Alignment Sensitivity

We first evaluate FAS by comparing its results to alignment sensitivity data simulated using LightTools. A 500- μm diameter, 0.22-NA step-index light guide (Polymicro Technologies FIP500550590; USA) was selected for this comparison. The light guide was first modeled in the software by creating a 20- m long cylindrical core made from silica glass, surrounded by another cylindrical tube representing the cladding. The material for each was set according to the manufacturer specifications to accurately reflect the index of refraction, absorption coefficient, and Fresnel reflection. A buffer of polyimide was created to surround the cladding to completely model the physical structure.

A 25.4- mm diameter uniform disk source was then created to model a well-collimated light source. The source emits collimated light (± 1 degree) at a wavelength of 652 nm to be consistent with the laser source used for the experimental measurements discussed in the following section. A 25.4- mm diameter lens, with a focal length of 60 mm was placed a distance of 30 mm from the disk source. The focal length was selected such that the light is focused within the numerical aperture of 0.22. Finally, the light guide structure is placed at the focal point of the lens (approximately 60 mm from the rear vertex), using the best-focus tool provided in the software. A detection surface is placed at the distal end of the light guide to measure the transmitted energy. A schematic of this model is shown in Fig. 3.

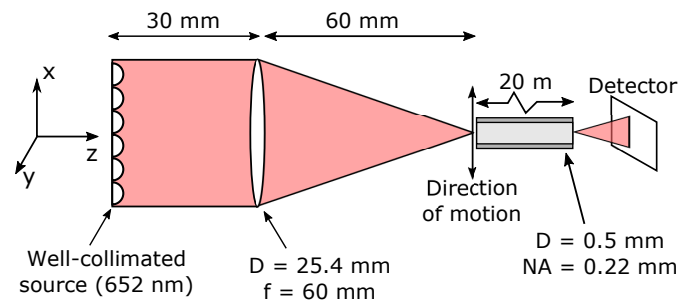


Fig. 3. Schematic of the model used to simulate the alignment sensitivity of a 0.5- mm diameter step-index light guide.

A macro was written to simulate the transmitted power as the light guide is laterally de-centered from the best-focus position,

for displacements ranging from $0\ \mu\text{m}$ to $1000\ \mu\text{m}$ in increments of $10\ \mu\text{m}$ along the local x -axis. The simulation was repeated for the best-focus position, as well as five defocus positions, incremented by $100\ \mu\text{m}$ along the local z -axis. For each case, the spot irradiance profile at the face of the fiber was saved to disk. The profile was then loaded into Python and a top-hat distribution function was generated with a radius of $250\ \mu\text{m}$. Using these two distributions, the FAS algorithm was used to compute the alignment sensitivity using Eq. (3). All simulations and computations were done on a computer with an Intel Core I-4710HQ CPU (2.50GHz) and 16GB DDR3L memory.

B. Physical Measurement of Alignment Sensitivity

B.1. Experimental Setup

We physically validated the FAS algorithm using a custom fiber characterization station (FCS, Fig. 4). The FCS is a multi-purpose fiber property measuring device that can inject spatially filtered and variable $F/\#$ light into an optical fiber while simultaneously imaging the fiber input face as well as the near and far field of the fiber output using high resolution cameras. This typically allows for precision study of optical fiber scrambling gain, modal noise, focal ratio degradation, and throughput. For this experiment, we used the FCS to reimaged a $10\text{-}\mu\text{m}$ pinhole, backlit by a 652-nm , 40-mW , fiber-fed, laser-driven light source (Toptica; Germany), onto the face of a circular optical fiber attached to a micron-precision position-controlled fiber stage. The input face of the fiber was $10\times$ magnified and imaged using a camera (Atik 450; UK). The light from the output of the optical fiber was simultaneously refocused onto a photodiode power sensor (Thorlabs S121C; USA) attached to a power meter with approximately 10-nW precision.

We first visually confirmed that the pinhole was focused and centered on the optical fiber face using the fiber-input camera and saved an image of the spot's spatial profile. A bright-field image, which is later used to establish a spatial scale, was also acquired by broadly illuminating the fiber core in reverse and once again imaging the fiber face. We then laterally displaced the fiber face (x -axis) at regular intervals of $10\ \mu\text{m}$ to a maximum of $300\ \mu\text{m}$, using the micrometer controls of the fiber input stage, and recorded the power meter reading for each position. The interval was reduced (to a minimum of $1\ \mu\text{m}$ increments) to provide a finer resolution when the transmission was observed to vary. We repeated these measurements after defocusing the reimaged pinhole by slightly distancing the pinhole from the collimation optics and taking an image of the defocused spot profile.

Using this process, we tested two different circular light guides. First is a $100\text{-}\mu\text{m}$ core diameter, 0.22-NA (Thorlabs M15L02; USA) optical fiber and second is a $550\text{-}\mu\text{m}$ core diameter, 0.22-NA dual-clad fiber (Thorlabs FG550UEC; USA). In the first case, a traditional top-hat function is used to represent the input face. Conversely, for the $550\text{-}\mu\text{m}$ light guide, we represent the input face as a two-step top-hat function to account for the additional transmittance caused by the dual cladding. In this case, the core transmittance is set at 1.0 and the inner cladding was measured at approximately 0.6 .

We then tested the robustness of the algorithm against two custom-made radially asymmetric light guides. First we tested a $200\text{-}\mu\text{m}$, 0.22-NA octagonal fiber surrounded by $672\text{-}\mu\text{m}$ cladding (CeramOptec; Germany) before investigating a $100\text{-}\mu\text{m} \times 300\text{-}\mu\text{m}$, 0.22-NA rectangular fiber surrounded by $660\text{-}\mu\text{m}$ cladding (CeramOptec; Germany). For each we tested both a

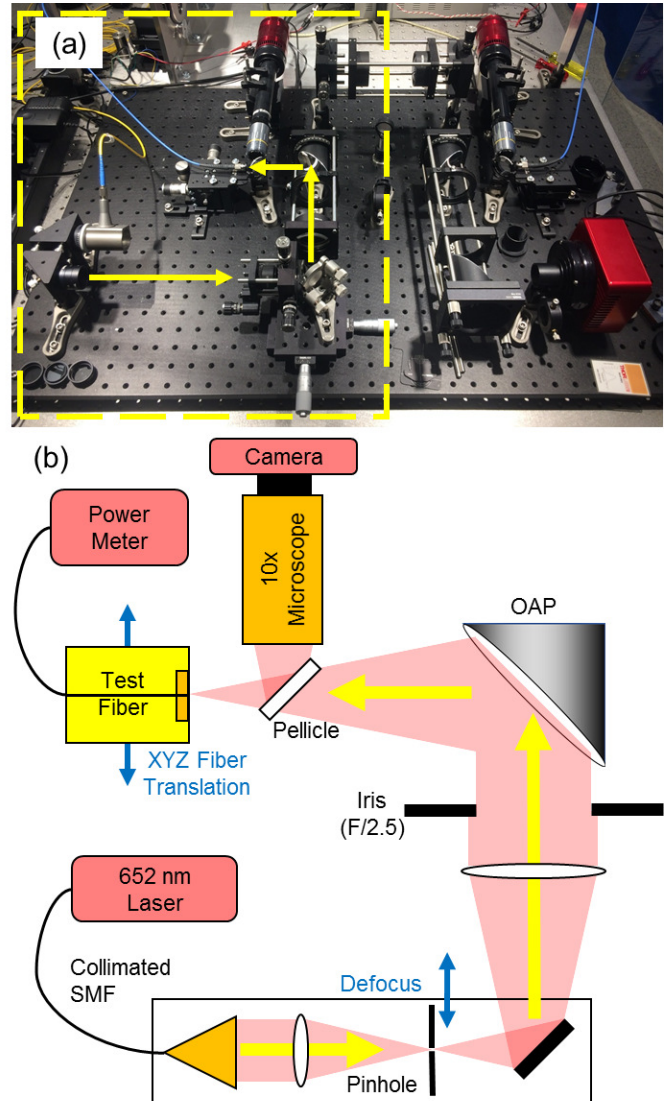


Fig. 4. Experimental setup of the fiber characterization station used to test the FAS algorithm. Panel (a) illustrates the full system, with a yellow box surrounding the components relevant to the fiber testing, while (b) provides a schematic of the components included in the yellow box.

focused spot and a defocused spot; additionally, we tested the octagonal fiber with a two-lobe spot produced by misaligning the beam injection system. For these tests, the fiber input face was represented by the image obtained with the fiber-input camera under bright-field illumination, as the more complex geometry and relative transmittance of the core and cladding was nontrivial to generate in software. Finally, we tested a non-Gaussian beam shape by removing the pinhole and replacing the laser input with a 100- μm LED multi-mode fiber (Polymicro Technologies; USA), which was re-imaged to a 60- μm spot. Coupling between two optical fibers is commonly found in spectroscopic applications; therefore, this test represents a more realistic scenario. This beam shape was tested with a 200- μm core diameter, 0.22-NA step-index fiber (Polymicro Technologies; USA) and a 550- μm core diameter, 0.22-NA step-index fiber (Thorlabs FG550UEC; USA). For both of these tests, the fibers were once again represented by a top-hat function generated in software.

B.2. Data Processing

The raw measured data were processed by first subtracting a dark measurement taken before the light source was activated. Then, the data are normalized to a value of 1.0 for the power reading taken with no misalignment. Using the spot irradiance profile saved using the fiber-input camera, the file was read into Python and input into the FAS algorithm to compute the theoretical alignment sensitivity. Finally, this result was rescaled along the x-axis using a conversion factor determined using the bright-field image. This was done by establishing the spatial distance corresponding to a single pixel, derived by dividing the known fiber core diameter by the number of pixels spanning the core in the acquired image.

C. Application to Tolerance a Coupling System

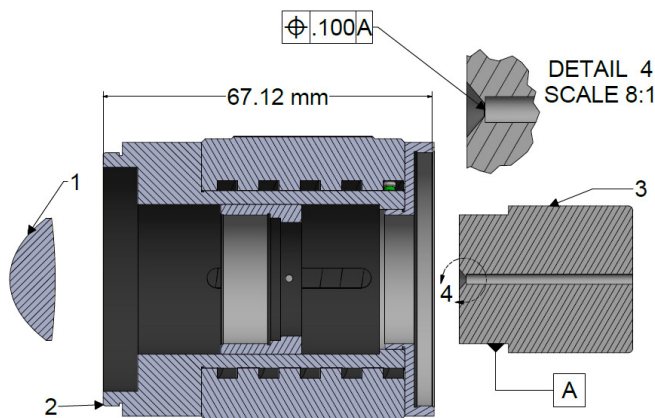


Fig. 5. Exploded cross-section of the final coupler design. A focusing lens (1) is inserted into an adjustable lens tube (2), which is connected to the custom mounting component (3). The FAS algorithm is used to tolerance the centration of the custom mounting component (4).

Following the physical verification with the FCS, we then demonstrated the practical application of FAS by applying it to determine the optimal tolerances for the centration of a custom light guide coupling system for the illumination fiber bundle of an endoscope (Polydiagnost Polyscope; Germany) [28]. The existing coupling is inefficient due to a decenter misalignment caused by a low tolerance. This is particularly problematic, as the

light guide must be re-aligned with each exchange of a disposable catheter between patients, leading to long alignment delays that inhibit clinical use. Therefore, an efficient and repeatable coupler assists in robust and streamlined clinical application.

The system focuses light from a semi-collimated LED source (Prismatix UHP-T-LED Series; Israel) into the illumination fiber bundle, which has a 1- mm core diameter and a numerical aperture of 0.67 (Fig. 5a). A custom mounting component was designed with a physical stop to axially fix the position the illumination fiber bundle (cross section: Fig. 5b). For the purpose of testing, a 75- mm focal length lens (Thorlabs AC254-075-A-ML; USA) is mounted in an adjustable lens tube (Thorlabs SM2NR1; USA), which is threaded to the end of the custom component to enable axial alignment consistently between fiber bundle exchanges.

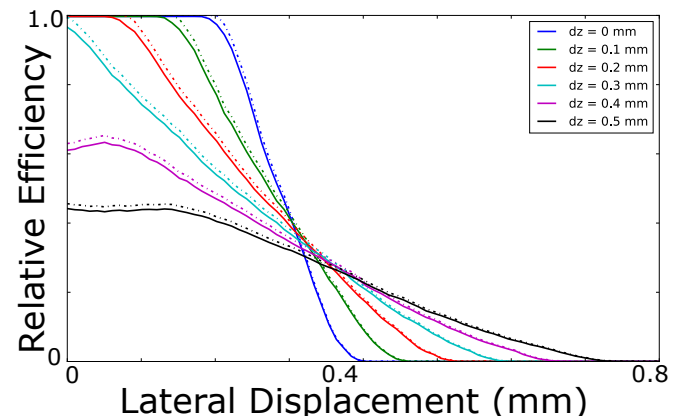


Fig. 6. Comparison between ray tracing simulations (solid lines) and the FAS algorithm (dashed lines) for various defocus positions. Both approaches show excellent agreement, indicating that FAS is a suitable replacement for modeling and simulation.

To determine the optimal centration tolerance on the custom component, the FAS algorithm was used to find the alignment sensitivity curve for the prescribed source and focusing lens. The source divergence was determined by measuring the change in beam diameter over a three-meter distance and the spot profile was generated in LightTools, which was then used as an input to the FAS algorithm. An estimate of 100 μm of defocus was used for the simulation, corresponding to the uncertainty in the axial alignment of the adjustable lens tube. The optimal centration tolerance was determined by inspecting the alignment sensitivity curve and finding the maximum lateral displacement that produces a relative transmission of unity.

Following fabrication, the coupling system was tested by inserting the Polyscope illumination fiber bundle into the custom mounting component, threading the system onto the Prismatix light source, and placing a photodiode detector (Newport 918D; USA) at the distal end of the illumination fiber. This was then compared with the maximum achievable transmitted power, measured by manually aligning the same fiber by translation (in x, y, z) until the transmitted power was maximized. This approach was taken to account for the additional losses in the system caused by the fill-factor of the fiber bundle, the absorption and reflection losses in the system, as well as any defects in the components.

4. RESULTS AND DISCUSSION

A. Simulated Alignment Sensitivity

The results from comparing the ray tracing simulations and the FAS algorithm show excellent agreement (Fig. 6). FAS yields a small (<5%), but consistent overestimate, indicative of a systematic error, which is not accounted for in the algorithm. A possible source of this error is the absorption of the fiber core and cladding, which is simulated in the ray tracing, but not accounted for in FAS. Other possibilities include cladding transmission, or that some information is lost due to the discretization of the spot profile applying the FAS algorithm, which could be mitigated by sampling the profile at a higher rate.

The FAS algorithm completed the computation in under three seconds for each defocus position, while ray tracing simulation took approximately 10 minutes. This is an improvement of over two orders of magnitude and FAS has the added benefit of providing a 2-dimensional map of alignment sensitivity, whereas the ray tracing simulations produce data in a single dimension only. While one dimension is sufficient to fully understand the behavior of rotationally symmetric systems, this property implies that FAS can be applied to systems lacking rotational symmetry, such as rectangular or octagonal light guides, which we test, or freeform light pipe systems.

B. Physical Measurement of Alignment Sensitivity

B.1. Radially Symmetric Fibers

Using the spot irradiance profile images obtained with the fiber-input camera (Fig. 7), the FAS algorithm was used to compute the alignment sensitivity and this was compared with the experimentally measured values. The results match extremely well for all cases (Fig. 8). Both the 100- μm and 550- μm fibers are shown to behave as predicted by FAS. In particular, it is noted that the 550- μm fiber (Fig. 8b,d) gives rise to non-standard behavior due to the additional transmittance caused by the dual-cladding geometry, which is accurately predicted by FAS by representing the fiber as a two-step top-hat function. Furthermore, for the cases with a severely defocused spot (Fig. 8c,d), FAS maintains high accuracy. These results indicate that FAS is a robust method to determine how the transmission of a light guide will depend on the lateral displacement, independent of the other system components and alignment errors.

B.2. Radially Asymmetric Fibers and Non-Gaussian Beam Profile

Once again using the spot irradiance profiles obtained with the fiber-input camera, the FAS algorithm was applied to compute the alignment sensitivity for the five test cases involving an octagonal and rectangular fiber. The results match well for all cases (Fig. 9). There is minimal disagreement (<5%) for the focused (Fig. 9a,c) and defocused (Fig. 9b,d) cases. We observe some discrepancy (10%) in the form of a dip between the measured and simulated values for the two-lobe spot (Fig. 9e); this could be caused by unexpected mode propagation behavior in the cladding, which the FAS algorithm does not consider.

The test cases with a non-Gaussian beam profile show excellent agreement (Fig. 9f,g). Both cases demonstrate very high agreement between the measured and simulated values (<5%). Testing a multi-mode fiber injection represents a realistic case that is found frequently in spectroscopic applications; taken together with the favorable results with radially asymmetric fibers indicates that the FAS algorithm is applicable to a wide range of beam profiles and fiber geometries.

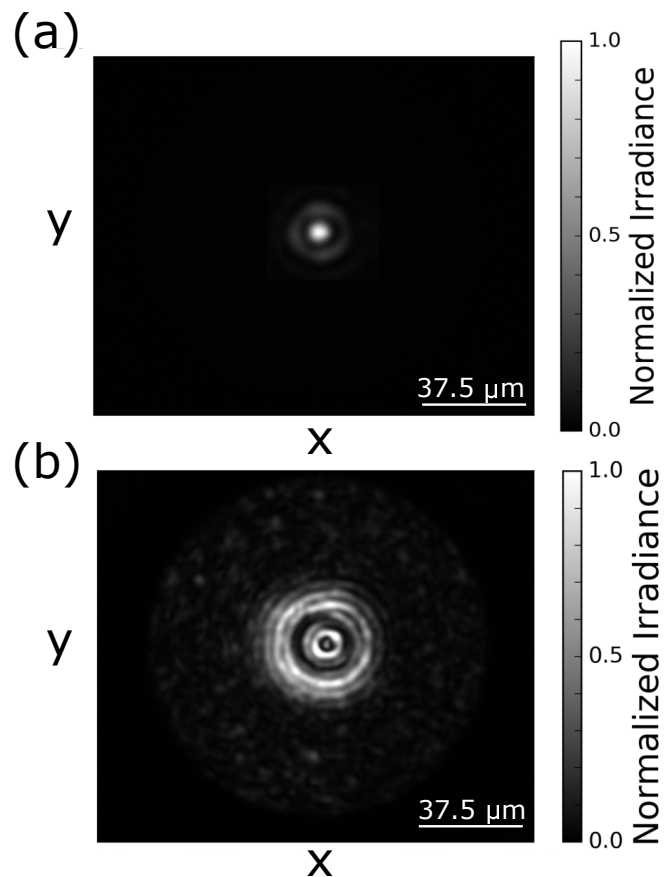


Fig. 7. Spot profile of a focused (a) and defocused (b) spot obtained by imaging the fiber face while testing the 100- μm diameter fiber. This profile is used to compute the alignment sensitivity with the FAS algorithm. The visible presence of noise in (b) is due to different normalization factors between the two images and also that (a) has been zero-padded to remove the majority of noise corruption.

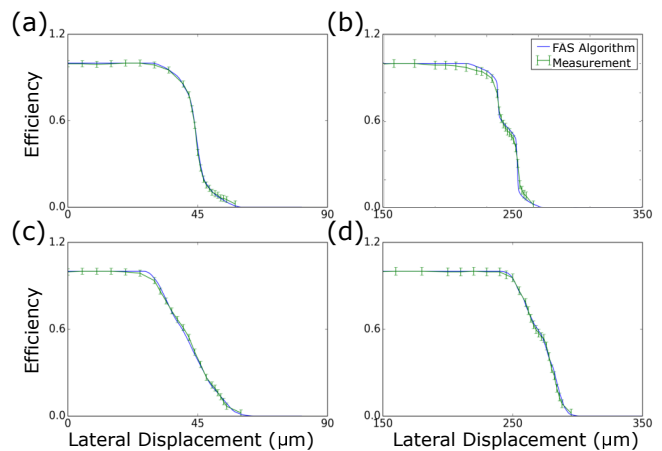


Fig. 8. Comparison between physical measurements and the FAS algorithm for a 100- μm light guide (focused spot: a, defocused: c) and a 550- μm light guide (focused spot: b; defocused: d).

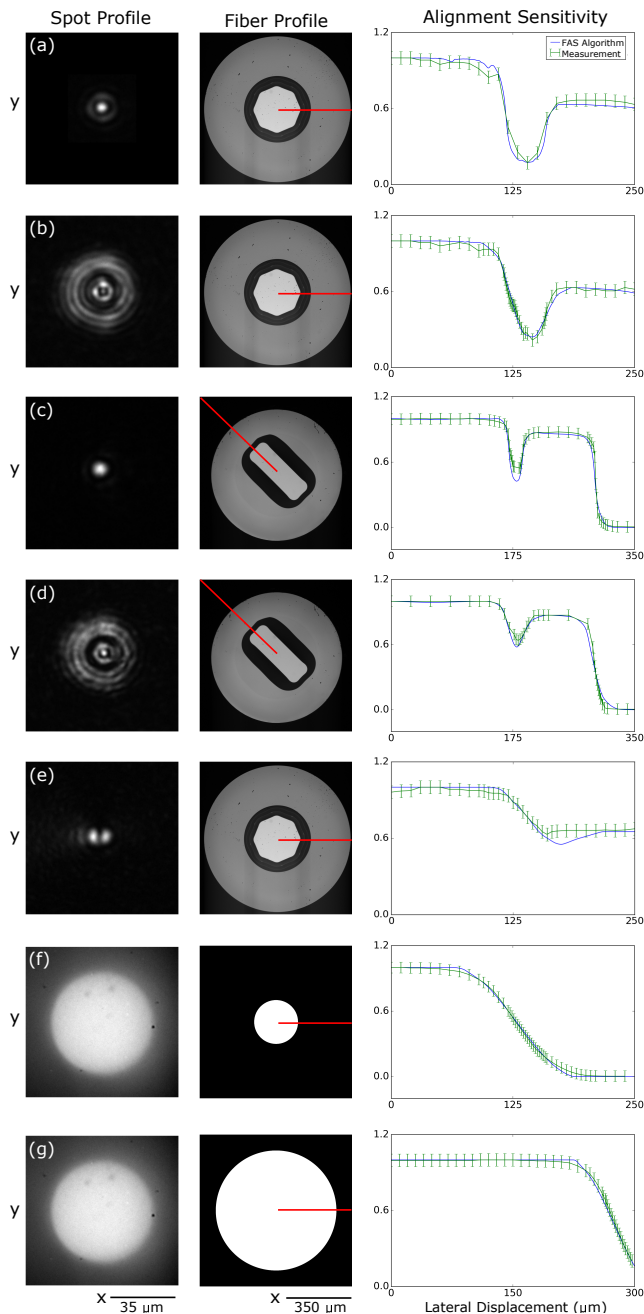


Fig. 9. Comparison between physical measurements and the FAS algorithm for an octagonal fiber (a: focused spot, b: defocused spot; e: two-lobe spot), a rectangular fiber (c: focused spot, d: defocused spot), and a multi-mode fiber injection spot (f: 200 μm diameter, g: 550 μm diameter). Shown in the right column is the spot profile; the central column represents the fiber profile, with a red line designating the dimension of misalignment; and the right column shows the measured (green line) and simulated results (blue line).

C. Application to Tolerance a Coupling System

When manually aligned for maximum transmission, the transmitted power through the tested light guide was measured as $164.02 \mu\text{W} \pm 5 \mu\text{W}$. The transmission with the custom mounting component was measured as $160.02 \mu\text{W} \pm 5 \mu\text{W}$. This demonstrates that the system performs within the specifications and thus validates FAS as a tolerancing technique. Considering the vast improvement in computation time over ray tracing, these results indicate that FAS provides both time and cost savings by providing a rapid means to determine the optimal tolerances, thus maximizing system performance while ensuring that the tolerances are not unnecessarily tight.

While these results are highly encouraging, we identify a number of topics for future investigation. These include examining the limit of validity for FAS in terms of the number of supported modes for a light guide. In addition, a theoretical examination of the behavior of mode coupling in the limit of many modes could yield important information regarding alignment sensitivity in a broader scope. Of further interest is to examine more extensively the robustness of FAS by testing freeform light pipe structures to validate that the accuracy is maintained for highly freeform systems. Finally, formulating a more sophisticated approach to extracting optimal tolerances from the alignment sensitivity curves would better inform the design and tolerancing process.

5. CONCLUSIONS

In this paper, a novel approach called the Fourier Alignment Sensitivity (FAS) algorithm is proposed to compute the alignment sensitivity of light guides, fiber bundles, and large-core optical fibers (LCOF) for the purpose of tolerancing coupling systems. The method involves using Fourier theory to compute the overlap integral between the incident light distribution and the light guide input face for a range of lateral misalignment. The sensitivity is first modeled in software and then measured using a characterization station for optical fibers. The FAS algorithm shows excellent agreement with both the measured and simulated results and improves over ray tracing simulation time by over two orders of magnitude. We then design and tolerance a coupling system for endoscopic illumination using the FAS algorithm to determine the optimal tolerances for centration. The system is tested for throughput and it is shown that the performance meets the specifications. These results indicate that FAS is an accurate approach to compute the alignment sensitivity, which enables a rapid and efficient determination of the optimal centration tolerances for light guide coupling systems. In addition to offering time and cost savings, a further benefit of FAS is the flexibility to extend to systems lacking rotational symmetry, such as non-circular optical fibers and light pipes. Hence, FAS is a flexible and robust approach, which has potential to widely inform system design and tolerancing by rapidly characterizing alignment sensitivity in systems that involve coupling to a light guide.

FUNDING INFORMATION

This material is based upon work supported by the National Science Foundation Graduate Research Fellowship Program under Grant No. DGE-1143953. Any opinions, findings, and conclusions or recommendations expressed in this material are those of the author(s) and do not necessarily reflect the views of the National Science Foundation. TWS is funded by the

NSF and the Winston Churchill Foundation of the United States. SEB is funded by CRUK (C14303/A17197, C47594/A16267 and C47594/A21102) and the European Union's Seventh Framework Programme (FP7/2007-2013) under grant agreement number FP7-PEOPLE-2013-CIG-630729. The Fiber Characterization Station was built with support from the Theodore Dunham, Jr. Grant of the Fund for Astrophysical Research, Inc.

ACKNOWLEDGMENT

We would like to thank Dr. John Koshel (University of Arizona) for simulation guidance and general illumination support, and Dale Waterhouse (University of Cambridge) for helping determine specifications for the Polyscope coupling system.

REFERENCES

1. H. Hamam and S. Guizani, "Optical Fiber Communications," in "Handbook of Computer Networks," vol. 1 (2011), pp. 692–707.
2. T. Li, "Advances in Optical Fiber Communications: An Historical Perspective," *IEEE Journal on Selected Areas in Communications* **1**, 356–372 (1983).
3. S. Personick, *Fundamentals of Optical Fiber Communications* (Academic Press, 1981).
4. J. Aceituno, S. F. Sánchez, F. Grupp, J. Lillo, M. Hernán-Obispo, D. Benitez, L. M. Montoya, U. Thiele, S. Pedraz, D. Barrado, S. Dreizler, and J. Bean, "CAFE: Calar Alto Fiber-fed Échelle spectrograph," *Astronomy & Astrophysics* **552**, A31 (2013).
5. S. Mahadevan, L. Ramsey, C. Bender, R. Terrien, J. T. Wright, S. Halverson, F. Hearty, M. Nelson, A. Burton, S. Redman, S. Osterman, S. Diddams, J. Kasting, M. Endl, and R. Deshpande, "The Habitable-Zone Planet Finder: A Stabilized Fiber-Fed NIR Spectrograph for the Hobby-Eberly Telescope," *Proc. SPIE* **9147**, 91471G (2014).
6. S. Perruchot, F. Bouchy, B. Chazelas, R. F. Díaz, G. Hébrard, K. Arnaud, L. Arnold, C. Centre, D. Physique, P. D. Marseille, D. Luminy, R. F. Diaz, G. Hebrard, G. Avila, X. Delfosse, I. Boisse, G. Moreaux, F. Pepe, Y. Richaud, A. Santerne, R. Sottile, D. Tezier, and D. Tézier, "Higher-precision radial velocity measurements with the SOPHIE spectrograph using octagonal-section fibers," *Proc. SPIE* **8151**, 815112 (2011).
7. B. A. Flusberg, E. D. Cocker, W. Piyawattanametha, J. C. Jung, E. L. M. Cheung, and M. J. Schnitzer, "Fiber-optic fluorescence imaging," *Nat. Methods* **2**, 941–950 (2005).
8. G. J. Tearney, S. a. Boppart, B. E. Bouma, M. E. Brezinski, N. J. Weissman, J. F. Southern, and J. G. Fujimoto, "Scanning single-mode fiber optic catheter-endoscope for optical coherence tomography," *Opt. Lett.* **21**, 543–545 (1996).
9. I. N. Papadopoulos, S. Farahi, C. Moser, and D. Psaltis, "High-resolution, lensless endoscope based on digital scanning through a multimode optical fiber." *Bio. Opt. Exp.* **4**, 260–70 (2013).
10. Newport, "Fiber Optic Basics," <https://www.newport.com/t/fiber-optic-basics> (2016).
11. R. Paschotta, "Multimode Fibers," https://www.rp-photonics.com/multimode_fibers.html (2008).
12. R. Paschotta, "V Number," https://www.rp-photonics.com/v_number.html (2008).
13. G. Rupprecht, "The exoplanet hunter HARPS: performance and first results," *Proc. SPIE* **5492**, 148–159 (2004).
14. Y. Jeong, J. Sahu, D. Payne, and J. Nilsson, "Ytterbium-doped large-core fiber laser with 1.36 kW continuous-wave output power." *Opt. Exp.* **12**, 6088–6092 (2004).
15. C. T. Bourn and C. A. Lemaire, "Fiber bundle combiner and led illumination system and method," <https://www.google.com/patents/US6290382> (2001).
16. K. Ishibashi, N. Shiraishi, and S. Oshiro, "Illumination optical system using optical fiber bundles," <https://www.google.com/patents/US4272156> (1981).
17. S. Santos, K. K. Chu, D. Lim, N. Bozinovic, T. N. Ford, C. Hourtoule, A. C. Bartoo, S. K. Singh, and J. Mertz, "Optically sectioned fluorescence endomicroscopy with hybrid-illumination imaging through a flexible fiber bundle," *J. Bio. Opt.* **14**, 30502 (2009).
18. X. Liu, Y. Huang, and J. U. Kang, "Dark-field illuminated reflectance fiber bundle endoscopic microscope." *J. Bio. Opt.* **16**, 046003 (2011).
19. F. Fournier and J. Rolland, "Optimization of freeform lightpipes for light-emitting-diode projectors." *App. Opt.* **47**, 957–66 (2008).
20. J. F. Van Derlofske, "Computer modeling of LED light pipe systems for uniform display illumination," *Proc. SPIE* **4445**, 119–129 (2001).
21. J. F. Van Derlofske, D. J. Lamb, and L. W. Hillman, "Computer Modeling of Illumination Systems for Automotive Displays," in "SAE Technical Paper," (SAE International, 1996).
22. RP Photonics Consulting GmbH, "RP Fiber Calculator," (2016).
23. F. Mauch, M. Gronle, L. Wolfram, and W. Osten, "Open-source graphics processing unit – accelerated ray tracer for optical simulation tracer for optical simulation," *Opt. Eng.* **52**, 053004 (2013).
24. J. Qin, "Hyperspectral Imaging Instruments," in "Hyperspectral Imaging for Food Quality Analysis and Control," (2010), pp. 129–172.
25. O. Wallner, P. J. Winzer, and W. R. Leeb, "Alignment tolerances for plane-wave to single-mode fiber coupling and their mitigation by use of pigtailed collimators," *App. Opt.* **21**, 637–643 (2002).
26. M. Blomqvist, M. Pålsson, O. Blomster, and G. Manneberg, "Fundamental-mode fiber-to-fiber coupling at high-power," *Proc. SPIE* **7193**, 71930F (2009).
27. P. Duhamel and M. Vetterli, "Fast fourier transforms: A tutorial review and a state of the art," *Signal Process.* **19**, 259–299 (1990).
28. M. J. Bader, C. Gratzke, S. Walther, B. Schlenker, D. Tilki, Y. Hocaoglu, R. Sroka, C. G. Stief, and O. Reich, "The PolyScope: a modular design, semidisposable flexible ureterorenoscopy system." *J. Endourology* **24**, 1061–1066 (2010).